ELSEVIER

PII: S0032-3861(97)10253-1

Polymer Vol. 39 No. 20, pp. 4785–4791, 1998

0032-3861/98/$19.00+0.00

Particle cavitation in rubber-toughened PMMA: experimental testing of the energy-balance criterion

D. S. Ayre* and C. B. Bucknall
Advanced Materials Department, Cranfield University, Bedford MK43 0AL, UK
(Received 3 July 1997; accepted 16 October 1997)

A programme of experiments is used to test the validity of the energy-balance model for rubber particle cavitation[1,2]. The yield behaviour of a transparent grade of rubber-toughened poly(methyl methacrylate) (RTPMMA) is investigated over a range of temperatures, in tension, compression and flexure. Differences between yield in tension and yield in compression are shown to affect flexural yield behaviour, and in particular the position of the neutral plane, which shifts towards the compression surface when the material cavitates in tension. The energy-balance model is used to calculate when cavitation is energetically possible, and the experimental observations at each temperature are compared with the predictions of the model. It is found that the release of energy is a necessary but not sufficient condition for cavitation, and that a small energy barrier at small void sizes exerts a controlling influence upon the cavitation process. © 1998 Elsevier Science Ltd. All rights reserved.

(Keywords: rubber-toughening; PMMA; cavitation)

INTRODUCTION

Previous papers introduced an energy-balance model for rubber particle cavitation in toughened plastics[1,2]. The model accounts qualitatively for a number of previously unexplained observations[3], including the relationship between particle size and impact strength, and the effects of rubber modulus upon toughness. The aim of the present study is to test the model more precisely, by comparing its quantitative predictions with experimental data. The test procedure chosen is flexural testing of RTPMMA.

The deformation behaviour of ductile polymers, and especially rubber-toughened plastics, is different in tension from that observed in compression for two reasons: firstly the moduli of polymers are strain-dependent[4]; and secondly their yield stresses are substantially lower in tension[5], especially when they contain rubber particles that cavitate in response to a dilatational stress[1]. The aims of the present study are to examine the effects of this asymmetry in properties upon yielding in flexure, and to use the results as a test of the energy-balance model.

In a typical metal, elastic moduli are effectively independent of strain. Consequently, when a metal specimen of rectangular cross-section is subjected to flexural loading, the midplane becomes a neutral plane separating tensile and compressive regions. As the load increases, the surfaces of the specimen reach their respective yield stresses, and plastic zones extend from these outer layers towards the central plane. Because the differences between tensile and compressive yield stresses are very small[6], the position of the neutral plane is unaffected by the onset of plasticity.

In polymers, by contrast, the neutral plane is always displaced by a small amount from the centre of the bar under flexural loading. This effect is always present, even at small strains, owing to the non-linear viscoelastic behaviour of polymers. However, the displacement becomes much larger when the material yields. In the present programme, the location of the neutral plane has been observed in specimens of a transparent grade of RTPMMA tested to the point of plastic collapse, and the results are used to calculate tensile and compressive yield stresses for RTPMMA over a range of temperatures.

* To whom correspondence should be addressed

THE FLEXURAL TEST

The position of the neutral plane and load at the point of total plastic collapse are obtained from experimental observations on specimens tested in bending. Tensile and compressive yield stresses can easily be calculated from flexural test data by considering the forces acting on the specimen.

In flexural tests a simply supported beam of span (S), width (B) and depth (D) is subjected to a central point force (P) (*Figure 1*). As the applied force is increased, the stresses acting at the compressive and tensile surfaces will increase to their maximum values Y_c (compressive yield stress) and Y_t (tensile yield stress). The two yield zones will then extend inwards until they meet. This defines the point of plastic collapse, where the system cannot sustain an increase in load, and a 'plastic hinge' forms at the (displaced) neutral plane indicated in *Figure 1* ($y = d$). At this stage the stress is constant throughout the compressed side, and equal to Y_c. Similarly the stress is constant throughout the tensioned side, and equal to Y_t.

Consider the forces acting on one half of the beam. As the beam is in equilibrium, the forces acting horizontally must be equal:

$$Y_c \times (D-d) \times B = Y_t \times d \times B$$

and

$$\frac{d}{D} = \frac{Y_c}{Y_c + Y_t} \quad (1)$$

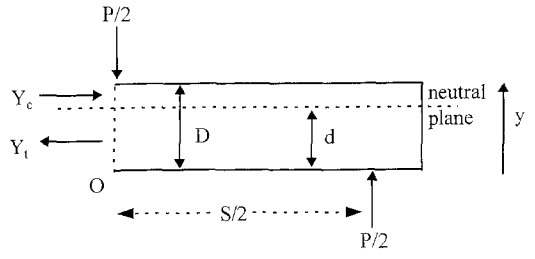

Figure 1 Forces acting on one half of a three-point bend specimen with a central load

Taking moments about O (*Figure 1*)

$$\frac{P}{2}\times\frac{S}{2}=B\times Y_c\times\int_d^D y\cdot dy-B\times Y_t\times\int_0^d y\cdot dy$$

$$\frac{PS}{4}=\frac{B}{2}(Y_cD^2-Y_cd^2-Y_td^2) \quad (2)$$

substituting in equation (1).

$$\frac{PS}{2BD^2}=\left(Y_c-\frac{Y_c^2}{Y_c+Y_t}\right) \quad (3)$$

When $Y_c = Y_t = \sigma_y$ this reduces to the standard beam equation[7]:

$$P=\frac{BD^2}{S}\sigma_y \quad (4)$$

From equation (1), it is obvious that the neutral plane will be displaced towards the compression face ($d > D/2$) when $Y_c > Y_t$.

EXPERIMENTAL

The material used for the study was a transparent rubber-toughened grade of PMMA, containing 40% by volume of three-stage core-shell modifier particles. The modifier particles comprised: a hard, lightly-crosslinked PMMA core, accounting for 40% of the modifier particle volume; a soft inner shell of lightly-crosslinked poly(butyl acrylate) copolymer rubber, grafted to the core and occupying about 50 vol% of the particle; and a grafted outer shell of PMMA making up the remaining 10%. The modifier particles were monodisperse, with a particle diameter of 0.22 μm. This material was known to exhibit cavitation of the rubber particles[8] under tensile test conditions at 23°C, causing it to whiten.

Test specimens were machined from plaques which were compression moulded at 200°C for 15 min, force cooled to 150°C, and then allowed to cool naturally. All testing was performed inside a temperature controlled cabinet using an Instron 6025 frame fitted with a 5 kN load cell and an Instron 5500 series controller. The specimens were conditioned to the test temperature for a minimum of 15 min in the cabinet before being tested.

A three-point bend (3PB) configuration was used for flexural testing[9]. Specimen dimensions of 12 mm (D) by 6 mm (B) by 120 mm (L) were adopted and a bending span of 100 mm (S) was chosen to minimise both shear in bending and buckling of the specimen (generally $6D < S < 12D$[10]). Each specimen was loaded at a crosshead speed of 1.4 mm/min until total plastic collapse. The position of the neutral plane was determined using a travelling microscope, viewing the specimen between crossed polars: RTPMMA exhibits photoelastic properties[11] which can be used to identify the neutral plane. The load at plastic collapse and the neutral plane position were then used to calculate yield stresses for compression (Y_c) and tension (Y_t) using equations (1) and (3).

Uniaxial tension and compression tests were carried out over a similar temperature range to provide yield data for comparison with the 3PB data. Tensile specimens with a 40-mm gauge length and a 3 × 5 mm cross-section were tested at a strain rate of 8×10^{-4} s^{-1} and compression specimens of 6 mm square base and 12 mm height were tested at the same strain rate in a compression cage. Frictional end effects were minimised by applying a lubricating grease (molybdenum disulphide) to the compression faces of the specimens.

RESULTS

Yield stresses, determined using flexural and uniaxial tests, are plotted against temperature in *Figures 2 and 3*. They show good agreement between the values of Y_c and Y_t obtained from the two types of test. To a first approximation, both Y_c and Y_t give linear plots consistent with Eyring theory[12], and both lines meet the abscissa at about 100°C, close to the T_g of PMMA.

Visual observation shows that at a strain rate of 5% min^{-1} the RTPMMA whitens during yielding in tension at all temperatures up to 55°C. The whitening is intense below 30°C, but becomes less pronounced at higher temperatures, and is barely detectable at 50°C. The transition in behaviour at ~55°C is accompanied by a shift in the final position of the neutral axis towards the mid-plane of the specimen, marking a change in the ratio Y_c/Y_t, as illustrated in *Figure 4*. All of these effects indicate that, at the chosen strain rate, cavitation of the rubber particles plays no significant part in tensile yielding at temperatures within 50 K of the T_g of PMMA.

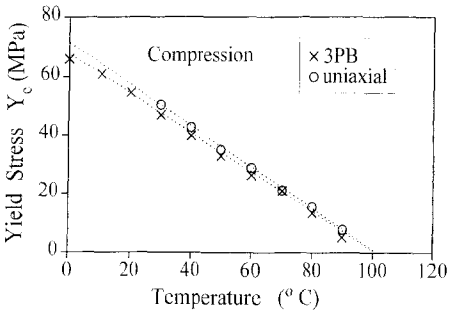

Figure 2 Effects of temperature on yield stress of RTPMMA in compression

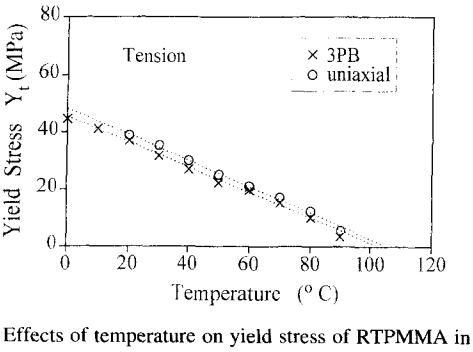

Figure 3 Effects of temperature on yield stress of RTPMMA in tension

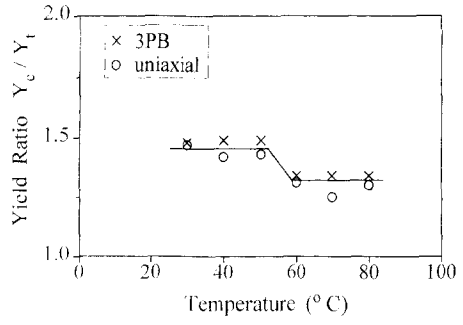

Figure 4 Effects of temperature on yield ratio Y_c/Y_t

It has been shown theoretically[2] that cavitation of monodisperse rubber particles can occur only if a critical volume strain, which is a function of particle size and morphology, is reached in the rubber phase. In the case of uniaxial tension, this sets a lower limit on the applied stress necessary to initiate voids. When RTPMMA specimens yield and deform before reaching this critical stress, they will not exhibit the whitening that is observed at 23°C. In the present series of experiments, the transition in deformation behaviour occurs at a uniaxial tensile yield stress of ~21 MPa, corresponding to a critical mean stress for cavitation of ~7 MPa.

DISCUSSION

These experiments on transparent RTPMMA provide a sensitive technique for defining the critical conditions for cavitation in rubber particles, and therefore constitute an important test of current theories of void formation. The volumetric strain energy necessary to form a void within a rubber particle is derived from two sources: differential thermal contraction and mechanical loading. Because of the large difference in coefficients of expansion between glassy polymers and elastomers, thermal stresses are always present in rubber-toughened plastics at all temperatures below T_{gm}, the T_g of the matrix. In some cases these internal stresses are sufficient to cause cavitation in the absence of external forces[13]. In the present experiments, both thermal and mechanical stresses contribute to void formation, and it is necessary to assess their separate contributions.

The first step is to consider the thermal stresses in a representative spherical element consisting of a simple rubber sphere of radius R enclosed in a PMMA shell of radius Q (*Figure 5*). The response of the PMMA shell to internal pressure P_R and external pressure P_Q can be calculated using the elastic analysis of Riesmann and Pawlik[14]. The radial displacement $x(q)$ within the PMMA matrix at a distance of q from the centre of the sphere is given by:

$$x(q) = \frac{(P_R R^3 - P_Q Q^3)q}{3K_m(R^3 - Q^3)} + \frac{(P_R - P_Q)R^3 Q^3}{4G_m(R^3 - Q^3)q^2} \quad (5)$$

where K_m and G_m are the bulk and shear moduli of the matrix.

For small strains, the volume strain, ΔV_{mR}, in the matrix shell at a radial distance R (the rubber–matrix interface) is:

$$\Delta V_{mR} = \frac{3x(R)}{R} = \frac{P_Q - P_R\phi}{K_m(1-\phi)} + \frac{3(P_Q - P_R)}{4G_m(1-\phi)}$$

$$= P_Q\left(\frac{4G_m + 3K_m}{4G_m K_m(1-\phi)}\right) - P_R\left(\frac{4G_m\phi + 3K_m}{4G_m K_m(1-\phi)}\right) \quad (6)$$

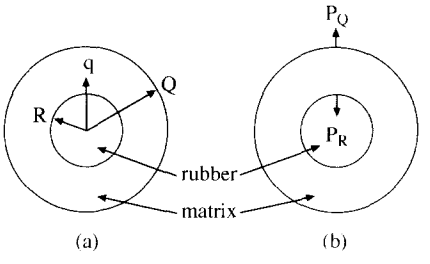

Figure 5 Composite spherical element showing (a) radical dimensions and (b) stresses acting on the matrix shell

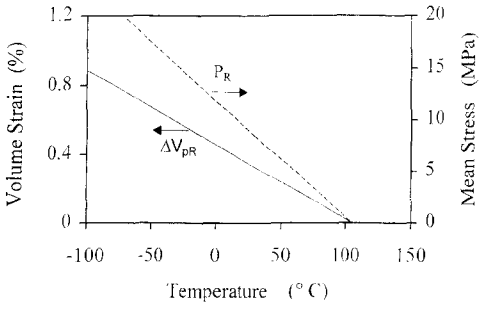

Figure 6 Effect of temperature on particle volume strain ΔV_{pR} and internal stress P_R, for unstressed RTPMMA ($P_Q = 0$), calculated using equation (9) with values quoted in *Table 1*

where $\phi = (R^3)/(Q^3)$ is the volume fraction of rubber particles in the toughened polymer.

The rubber acts as a simple sphere under external (negative) pressure, so the volume strain of the rubber particle is simply:

$$\Delta V_{pR} = \frac{P_R}{K_p} \quad (7)$$

where K_p = bulk modulus of the rubber particle. When the system is at temperature T, the strain mismatch caused purely by the difference between the volume coefficients of thermal expansion β_m and β_p will be $\Delta T(\beta_m - \beta_p)$, where $\Delta T = T - T_{gm}$. As there is good adhesion at the particle/matrix interface, this thermal volume strain mismatch will be equal to $(\Delta V_{mR} + \Delta V_{pR})$. Taking account of the differences in sign between the two volume strains:

$$\Delta T(\beta_m - \beta_p) = \Delta V_{pR} - \Delta V_{mR} \quad (8)$$

Substituting for ΔV_{pR} and ΔV_{mR}

$$\Delta T(\beta_m - \beta_p) = P_R\left(\frac{1}{K_p} + \frac{4G_m\phi + 3K_m}{4G_m K_m(1-\phi)}\right) - P_Q\left(\frac{4G_m + 3K_m}{4G_m K_m(1-\phi)}\right) \quad (9)$$

Equation (9) shows that P_R, the internal stress acting on the rubber particle, arises in two ways: (a) from thermal contractions, represented by the term in ΔT; and (b) from mechanical loading of the system, represented by the term in P_Q. The stress P_R and the volume strain ΔV_{pR} within the rubber phase, which are directly proportional to ΔT at fixed external pressure P_Q, are depicted in *Figure 6* for the condition $P_Q = 0$.

Having calculated the stresses acting on both the rubber particle and the surrounding matrix, the next step is to calculate the energy changes that result from cavitation of the rubber. These are dependent upon the choice of

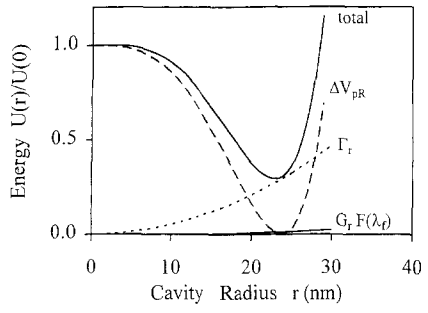

Figure 7 Energy changes in a rubber particle during cavity growth (from equation (10)). ΔV_{pR} = Rubber volume strain energy; Γ_r = surface energy; $G_r F(\lambda_f)$ = stretching energy

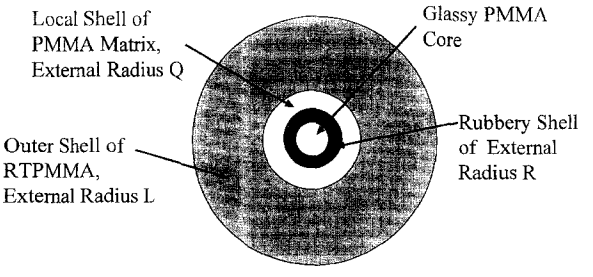

Figure 8 The four-stage system used to model changes in volume strain and energies during void formation in the rubber shell

boundary conditions. The simplest case, as discussed in earlier papers[1,2], involves first increasing the particle radius from its unstressed value R_0 to its current value R, and then holding it constant during cavitation. Under these conditions, there is no interchange of energy between particle and matrix as the void expands, and we can write[1,2]:

$$U(r) = \frac{2}{3}\pi R^3 K_p \left(\Delta V_{pR} - \frac{r^3}{R^3}\right)^2 + 4\pi r^2 \Gamma_r + 2\pi r^3 G_r F(\lambda_f) \tag{10}$$

where r = radius of void; ΔV_{pR} = volume strain of rubber particle; Γ_r = surface energy of rubber; G_r = shear modulus of rubber; $F(\lambda_f)$ = a function of the rubber extension ratio λ_f at failure[1].

From equation (10), it can be seen that the energy of the rubber particle is determined by three terms: the residual volumetric strain energy, the surface energy of the cavity, and the local membrane stretching around the void. Each of these energy terms is shown separately in *Figure 7*, for a homogeneous rubber particle of diameter 0.22 μm, having the properties listed in *Table 1*. As the cavity radius r increases, the initial volume strain in the rubber phase is gradually relieved and finally reaches zero. At this point the rubber achieves its equilibrium unstressed density: further growth of the void causes compressive strain in the rubber, and an increase in strain energy. Because of the contributions from surface energy and membrane stretching, the minimum in overall energy $U(r)$ occurs a little earlier than the minimum in volumetric strain energy.

The imposed volume strain ΔV_{pR} in equation (10) is determined by the combination of thermal contraction and mechanically generated strains experienced by the particle. If the particle radius R and temperature interval ΔT are large enough, the rubber particles may cavitate simply as a result of cooling, without applying external stresses. More typically, the critical volume strain includes both thermal and mechanical contributions.

A simple modification enables equation (10) to be applied to particles in which a rubbery shell encloses a rigid thermoplastic core, as in a typical RTPMMA (*Figure 8*). From electron microscope evidence, voids are known to form in the rubbery shell, and their *initial* development is assumed here to be governed by the same surface energy and membrane stretching terms as for a homogeneous rubber particle having the same properties as the rubbery shell. However, the leading term in equation (10), which involves the bulk modulus of the particle, must take account of the rigid core, which alters the volume strain energy. A straightforward approach to this problem is to calculate the strain energy in the same way as for a homogeneous particle, but to use an effective bulk modulus K_p for the multi-layered particle. Similarly, the volume strain due to thermal contraction can be calculated using an effective coefficient of volumetric expansion β_p.

Boyce et al.[15] obtained expressions for these quantities using the method of Chow[16,17], as follows:

$$K_p = K_r \left\{ 1 + \frac{\left[\frac{K_c}{K_r} - 1\right]\phi_c}{1 + \left[\frac{K_c}{K_r} - 1\right][1-\phi_c]\left[\frac{1+\nu_r}{3(1-\nu_r)}\right]} \right\} \tag{11}$$

$$\beta_p = \beta_r \left\{ 1 + \frac{\frac{K_c}{K_r}\left[\frac{\beta_c}{\beta_r} - 1\right]\phi_c}{1 + \left[\frac{K_c}{K_r} - 1\right]\left[(1-\phi_c)\left[\frac{1+\nu_r}{3(1-\nu_r)}\right] + \phi_c\right]} \right\} \tag{12}$$

where the subscripts c and r refer to the rigid core and the rubbery shell respectively, and ϕ_c is the volume fraction of the core material with respect to the particle. In the present

Table 1 Material properties assigned to the rubber-toughened PMMA

	Matrix	Rubber	Rubber particle
Bulk Modulus, MPa	$K_m = 4000$	$K_r = 2000$	$K_p = 2600$
Shear Modulus, MPa	$G_m = 1100$	$G_r = 0.1$	
Radius, μm	$Q = 0.15$	$R = 0.11$	$R = 0.11$
Volumetric Coefficient of Thermal Expansion, K^{-1}[a]	$\beta_m = 2.5 \times 10^{-4}$	$\beta_r = 6 \times 10^{-4}$	$\beta_p = 4.4 \times 10^{-4}$
Surface Energy, J m^{-2}		$G_r = 0.03$	
Rubber Extension Ratio Function		$F(\lambda_f) = 1$	
Poisson's Ratio	$\nu = 0.37$	$\nu_r = 0.49992$	
Volume Fraction of Rubber Particle Core			$\phi_c = 0.45$

[a]Data from Ref. [19]

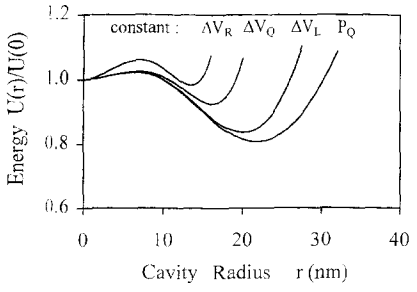

Figure 9 Effect of boundary conditions on the energy-balance curve, calculated using equations (5) and (10), and an initial rubber particle volume strain of 0.36%

programme, effective physical constants for the rubber particles have been calculated using equations (11) and (12). The properties assigned to the rubber and resulting values of K_p and β_p are given in *Table 1*.

In preparing this table, the shear and bulk moduli of PMMA were calculated using Poisson's ratio = 0.37 and tensile modulus = 3.1 GPa at 23°C[18]. No direct data were available for butyl acrylate copolymer rubber, but as the bulk modulus of many elastomers is close to 2 GPa, this value was chosen[19]. The rubber is expected to have a relatively low shear modulus because it is a saturated polymer and has a low level of crosslinking. Chain entanglement slip-links also contribute to modulus[20] as does physical crosslinking due to grafting at the PMMA/rubber interface[21]. Calculations show that variations in shear modulus G_r between 0.01 and 0.20 MPa do not affect $U(r)$ in equation (10) significantly, and a value of 0.1 MPa was therefore chosen for the present analysis.

The boundary condition used in the preceding discussion, defined by a constant particle radius R (and hence constant *particle* volume strain ΔV_{pR} as the void expands), makes it easier to explain the basic principles of the model, and to calculate energies, but results in a serious underestimate of the energy available to the growing void. Cavitation causes an increase in the volume compliance of the particle, so that its radius R increases as the void is formed. A previous paper, using a combination of equations (5) and (10), showed that the additional energy released by the matrix at this stage substantially alters the relationship between $U(r)$ and r^2: for any given initial particle volume strain ΔV_{pR}, the overall result is to shift the energy minimum to lower energies and larger void radii, as illustrated in *Figure 9*, which shows four curves corresponding to four different boundary conditions. The curve labelled ΔV_R refers to the condition R = constant, as discussed above. The curve labelled ΔV_Q includes energy inputs from a surrounding shell of matrix (*Figure 5a* and *Table 1*), where the radius of the shell, Q, is held constant during cavitation. Label P_Q indicates that the normal stress P_Q acting on the surface of the same shell, at radius Q, was kept constant during cavitation. These three cases are discussed in a previous paper[2]. The fourth curve, labelled ΔV_L, was obtained by applying equation (5), in combination with equation (10), to the four-stage model illustrated in *Figure 8*, where the matrix shell of radius Q is surrounded by a shell of external radius L, where $L \gg Q$. This outer shell is assigned the average properties of the rubber-toughened polymer: bulk modulus K_L = 3500 MPa and shear modulus G_L = 800 MPa. As L is so large, the boundary conditions ΔV_L = constant and P_L = constant give essentially the same curve of $U(r)$ against r. *Figure 9* shows that this curve, which is more representative of normal test conditions, lies between those calculated for constant volume ΔV_Q and for constant applied stress P_Q on the local matrix–particle element.

Table 2 Experimental yield results and calculated energy maxima during cavity growth

Temperature (°C)	Yield Stress (MPa)	Mean Stress (MPa)	Energy Max (aJ[a])	Cavity radius (nm)
30	35.4	11.8	1.0	2.7
40	30.0	10.0	1.35	3.3
50	24.6	8.2	2.0	4.1
60	21.0	7.0	3.0	5.0
70	16.8	5.6	5.2	6.7
80	12.0	4.0	13	11.3

[a]1 attoJoule (aJ) = 10^{-18} J

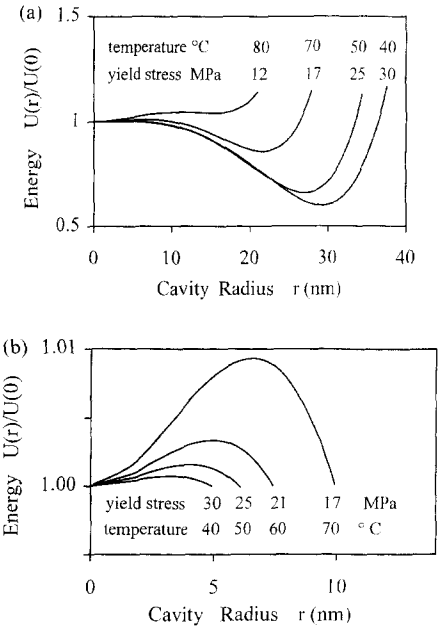

Figure 10 Energy-balance curves for experimental yield conditions, emphasising (a) the energy minima and (b) the energy maxima at small r. Yield stresses rounded to the nearest integer. See *Table 2* for exact data

The principles outlined above were used to compare experimental data with the predictions of the energy-balance model. *Table 2* lists the tensile yield stresses obtained experimentally in uniaxial tests between 30° and 80°C, and the corresponding mean stresses at yield. These data were used to calculate, at each combination of temperature and yield stress, the thermal contraction strains and energy interactions between matrix, rubber and void, using equations (5), (9)–(12), for a RTPMMA with the composition and properties given in *Table 1*. The chosen values of Q and R represent a typical fracture-resistant polymer with a particle volume fraction of 0.40. For purposes of these calculations, the T_g of PMMA was taken as 105°C.

The resulting energy curves are presented in *Figure 10*. It can be seen that the maximum stresses and volume strains reached at 80°C are not high enough to cause cavitation: at no point does the energy $U(r)$ fall below its original value $U(0)$, and cavitation is therefore thermodynamically impossible. On the other hand, the condition $U(r)_{min} < U(0)$ is satisfied at 70°C, and indeed appears to be applicable at all temperatures below 78°C. As the RTPMMA specimens

show no evidence of cavitation above about 55°C, it is clear that the thermodynamic criterion is a necessary but not sufficient condition for void formation in the rubber particles. At 70° and 60°C, the rubber particles are in a metastable state with respect to cavitation when the polymer reaches its yield point.

An obvious explanation for these observations is to be found in *Figure 10b*. The energy of the particle–matrix system reaches an energy maximum at small void sizes, essentially because the surface energy term, in Γ, has a disproportionate effect on the energy of the void at this stage. Such an energy barrier introduces a rate-controlling step into the cavitation process. For most processes involving an activation energy, rates increase with increasing temperature because more thermal energy is available to surmount the energy barrier. In the present case, however, thermally-activated cavitation occurs more easily at lower temperatures, where the RTPMMA is able to reach higher stresses and the height of the energy barrier is consequently reduced.

Similar energy maxima, also arising from surface energy effects, occur in crystallization and in the nucleation of bubbles beneath the surface of a boiling liquid. The pressure required to expand a bubble comes from the positive internal pressure of the vapour, whereas void expansion in rubber particles is driven by negative external pressure imposed on the toughened polymer, but the two cases are closely analogous.

Increasing the strain rate has a similar effect to lowering the temperature: at a fixed temperature, there is a transition from non-dilatational yielding to yielding with cavitation, as the yield stress of PMMA increases in accordance with Eyring kinetics[12]. This effect has been observed at 23°C in RTPMMA by Schirrer et al.[22], who defined a critical strain rate below which particle cavitation is not observed.

There are obvious difficulties in developing experimental methods for direct observation of the activated cavitation step in strained rubber particles. Firstly, the concentration of voids will necessarily be very small at the initiation stage, as opposed to the subsequent growth stage: a volume strain of 1%, applied to a toughened polymer with the relatively high rubber content of 20%, could result in an overall void content of up to 0.2%, under conditions where every particle has cavitated, and there is no further expansion of the voids. The best way to avoid the complications arising from expansion of cavitated particles would be to generate voids simply by cooling. As noted earlier, the dilatational energy available to the rubber particles as a result of differential thermal contraction is often sufficient to do this before the rubber reaches its glass transition temperature.

There are several methods for observing features with the expected dimensions of newly-formed, stable voids, which are in the order of 50 nm. The most effective techniques are neutron scattering and small-angle X-ray scattering (SAXS). However, these might not be effective in studying the transformation of 'free-volume' elements into stable voids. The most promising method for observing this process is positron annihilation lifetime spectroscopy, which is able to detect 'holes' with linear dimensions between 0.1 and 0.5 nm[23]: larger holes are not recognised because the distance over which *ortho*-positronium can interact with matter is relatively small. One observation that suggests the formation of true voids by coalescence of distributed 'free volume' is reported by Liu *et al.*[24], who in fatigue experiments on polycarbonate found that the positron annihilation lifetime increased and the intensity of the annihilation signal decreased as the stress amplitude was raised. It is not unreasonable to suggest that the distribution of intermolecular spacings in strained rubber particles might change in a similar way over a period of time, stimulated by thermal energy fluctuations.

In view of the problems outlined above, indirect methods for following activated cavitation in the rubber phase are likely to assume increasing importance in the near future. Schirrer *et al.* have used light scattering techniques to observe void growth in the rubber phase of a transparent grade of rubber-toughened PMMA[22]. Another indirect indicator of particle cavitation is a shift in the tan δ peak associated with the rubber T_g. With increasing volume strain (and hence free volume), the tan δ peak shifts to lower temperatures. However, once a void forms the volume strain in the rubber will be released as the particle reverts to its equilibrium density, and the peak will move to a higher temperature. This can sometimes result in splitting of the tan δ peak, as reported by Morbitzer *et al.*[13]

CONCLUSIONS

This work has demonstrated that flexural testing can be used to determine the tensile and compressive yield stresses of polymers simultaneously by measuring the position of the neutral plane. The technique lends itself to the study of yield mechanisms over a range of temperatures and strain rates, and is particularly effective in detecting transitions from one tensile yield mechanism to another. It works best in transparent polymers with suitable strain-optical properties. Initial work with RTPMMA over a range of temperatures, at a constant strain rate of 5% min^{-1}, has revealed a neutral plane shift at ~55°C. This shift is associated with a transition from cavitating to non-cavitating yielding under tension.

These observations are consistent with the energy-balance model for cavitation of rubber particles[1,2]. The volume strain energy responsible for void formation in the rubber phase is generated in two ways: (a) differential thermal contraction from the T_g of PMMA at 105°C, and (b) mechanical loading. These contributions to the strain energy, together with the core-shell structure of the rubber particles, are taken into account in calculating the energy balance under specific conditions. The case of most interest at each temperature is the tensile yield point, where the material reaches its maximum stress. Above 55°C, the RTPMMA used in this study is able to yield at stresses below those required to initiate cavitation in the rubber particles. However, as the temperature is reduced below 55°C, the increasing yield stress of the PMMA matrix, combined with the increasing thermally-induced stresses, causes cavitation before yield.

From the observed position of the transition in RTPMMA, it is clear that a simple thermodynamic criterion based on the principles outlined at the beginning of the *Discussion* section does not accurately represent the cavitation behaviour of rubber particles. The simple energy-decrease criterion predicts a transition at ~78° rather than 55°C. To explain this discrepancy, it is necessary to introduce a new criterion, which takes account of the small energy maximum that occurs in the initial stages of void nucleation. Because of the form of equation (10), the height of the energy barrier decreases with increasing volume strain, and hence with increasing yield stress. The energy barrier to cavitation at the yield point is therefore progressively reduced as the temperature is lowered.

Thus the present study has shown how flexural tests can be used as a sensitive method for defining critical conditions for rubber particle cavitation in at least one class of rubber-toughened polymers, and has identified void nucleation as a rate-controlling step. There are close similarities between void formation and homogeneous nucleation of crystals from melt or solution, which probably extend to the underlying kinetics of the two processes.

ACKNOWLEDGEMENTS

The authors thank the Engineering and Physical Research Council (GR/K24703) for financial support of this project, and Rohm and Haas for providing the toughened material.

REFERENCES

1. Lazzeri, A. and Bucknall, C. B., *J. Mater. Sci.*, 1993, **28**, 6799.
2. Bucknall, C. B., Karpodinis, A. and Zhang, X. C., *J. Mater. Sci*, 1994, **29**, 3377.
3. Bucknall, C. B., in *The Physics of Glassy Polymers*, 2nd edn., eds. R. N. Haward and R. J. Young. Chapman & Hall, London, 1997.
4. Ward, I. M., *Mechanical Properties of Solid Polymers*, 2nd edn, Ch. 9. J. Wiley & Son, Chichester, 1983.
5. Ward, I. M., *Mechanical Properties of Solid Polymers*, 2nd edn, Ch. 11. J. Wiley & Son, Chichester, 1983.
6. Spitzig, W. A., Sober, R. J. and Richmond, O., *Met. Trans.*, 1976, **7A**, 1703.
7. Williams, J. G., *Stress Analysis of Polymers*, 2nd edn, Ch. 4. Ellis Horwood Ltd, Chichester, 1980.
8. Lovell, P. A., McDonald, J., Saunders, D. E. J., Sherratt, M. N. and Young, R. J., *Plast. Rubber Compos. Proc. Appl.*, 1991, **16**, 37.
9. A.S.T.M. D790, *1994 Annual Book of ASTM Standards*, Vol. 08.01. American Society for Testing and Materials, Philadelphia, PA.
10. Davies, H. E., Troxell, G. E. and Hauck, G. F. W., *The Testing of Engineering Materials*, 4th edn. McGraw-Hill, New York, 1982.
11. Jessop, H. T. and Harris, F. C., *Photoelasticity, Principles and Practice*. Cleaver-Hume Press Ltd., London, 1949.
12. Eyring, H., *J. Chem. Phys.*, 1936, **4**, 283.
13. Morbitzer, L., Kranz, D., Humme, G. and Ott, K. H., *J. Appl. Polym. Sci.*, 1976, **20**, 2691.
14. Reismann, H., and Pawlik, P. S., *Elasticity: Theory and Applications*, Ch. 5. Wiley, New York, 1980.
15. Boyce, M. E., Argon, A. S. and Parks, D. M., *Polymer*, 1987, **28**, 1680.
16. Chow, T. S., *J. Polym. Sci. Polym. Phys. Edn.*, 1978, **16**, 959.
17. Chow, T. S., *J. Polym. Sci. Polym. Phys. Edn.*, 1978, **16**, 967.
18. Naqui, S. I. and Robinson, I. M., *J. Mater. Sci*, 1993, **28**, 1421.
19. Brandrup, J. and Immergut, E. H., *Polymer Handbook*, 3rd edn. Wiley, New York, 1989.
20. Edwards, S. F. and Vilgis, T., *Polymer*, 1986, **25**, 483.
21. Rohm and Haas, British Patent 1414187, 1975.
22. Schirrer, R., Fond, C. and Lobbrecht, A., *J. Mater. Sci.*, 1996, **31**, 6409.
23. Jean, Y. C., *Microchem. J.*, 1990, **42**, 72.
24. Liu, L. B., Gidley, D. and Yee, A. F., *J. Polym. Sci. Polym. Phys. Edn.*, 1992, **30**, 231.